Geophysical Research Letters

RESEARCH LETTER
10.1029/2021GL097108

An Extreme High Temperature Event in Coastal East Antarctica Associated With an Atmospheric River and Record Summer Downslope Winds

John Turner[1], Hua Lu[1], John C. King[1], Scott Carpentier[2], Matthew Lazzara[3], Tony Phillips[1], and Jonathan Wille[4]

[1]British Antarctic Survey, Natural Environment Research Council, Cambridge, UK, [2]Bureau of Meteorology, Hobart, TAS, Australia, [3]Madison Area Technical College and University of Wisconsin-Madison, Madison, WI, USA, [4]University of Grenoble, Grenoble, France

Key Points:

- Sustained horizontal warm advection toward the coast of East Antarctic via an atmospheric river led to marked warming
- Downslope surface winds of record strength for the summer resulted in descent and adiabatic warming inland of the coast
- Extremely strong lower tropospheric easterly winds carried the warm air westwards leading to ice melt and record high surface temperatures

Supporting Information:

Supporting Information may be found in the online version of this article.

Correspondence to:

J. Turner,
jtu@bas.ac.uk

Citation:

Turner, J., Lu, H., King, J. C., Carpentier, S., Lazzara, M., Phillips, T., & Wille, J. (2022). An extreme high temperature event in coastal East Antarctica associated with an atmospheric river and record summer downslope winds. *Geophysical Research Letters*, *49*, e2021GL097108. https://doi.org/10.1029/2021GL097108

Received 20 NOV 2021
Accepted 28 JAN 2022

Author Contributions:

Conceptualization: John Turner
Data curation: Matthew Lazzara, Tony Phillips, Jonathan Wille
Formal analysis: John Turner, Hua Lu, John C. King
Methodology: John Turner, John C. King, Scott Carpentier, Matthew Lazzara, Tony Phillips, Jonathan Wille
Software: Tony Phillips, Jonathan Wille
Writing – original draft: John Turner

Abstract High surface temperatures are important in Antarctica because of their role in ice melt and sea level rise. We investigate a high temperature event in December 1989 that gave record temperatures in coastal East Antarctica between 60° and 100°E. The high temperatures were associated with a pool of warm lower tropospheric air with December temperature anomalies of >14°C that developed in two stages over the Amery Ice Shelf. First, there was near-record poleward warm advection within an atmospheric river. Second, synoptically driven downslope flow from the interior reached unprecedented December strength over a large area, leading to strong descent and further warming in the coastal region. The coastal easterly winds were unusually deep and strong, and the warm pool was advected westwards, giving a short period of high temperatures at coastal locations, including a surface temperature of 9.3°C at Mawson, the second highest in its 66-year record.

Plain Language Summary The Antarctic continent contains 90 percent of the world's freshwater ice, so any significant melt has serious implications for sea level rise. To date, most ice loss has occurred when warm ocean currents melt coastal ice from below. However, the higher air temperatures predicted for the coming decades are expected to increase surface melt, leading to an additional contribution to sea level rise. We present a case study of an event that occurred in coastal East Antarctica during December 1989 that illustrates how surface temperatures can rise to record levels leading to significant surface ice melt. The event unfolded in two stages. First, a narrow band of warm, moist air arrived in the coastal region from lower latitudes as an "atmospheric river", raising the temperature to a high, but not extreme level. Second, winds of record summer strength flowed from the interior of the Antarctic to the coastal region, drawing air down to lower levels of the atmosphere. This led to warming of the coastal air through compression, with it reaching 9.3°C at the Australian Mawson station, which was the second highest surface temperature in the 66-year record.

1. Introduction

During the twenty-first century, the Antarctic ice sheet could make a significant contribution to sea level rise. If atmospheric and ocean temperatures continue to increase, it will lead to greater ice melt at the coastal fringes and acceleration of the ice streams descending from the interior (Bamber et al., 2019; Levermann et al., 2020; Nowicki & Seroussi, 2018). Since the 1970s there has been growing concern regarding ice loss from West Antarctica (Dutrieux et al., 2014; Turner et al., 2017). Here there has been grounding line retreat and thinning of the ice streams as warm waters melted the ice from below (Park et al., 2013; Pritchard et al., 2012).

Recently, there has been a focus on the sea level contribution from East Antarctica, with a suggestion that the East Antarctic Ice Sheet has been a major contributor to sea level rise over the last four decades (Rignot et al., 2019). Here ice loss was linked to basal melting of ice shelves by warm Circumpolar Deep Water (Herraiz-Borreguero et al., 2015). Surface melting on ice shelves promotes rapid retreat and break-up of the shelves, which then leads to accelerated loss of grounded ice (Tedesco, 2009). While the magnitude of East Antarctic surface melt is currently modest, climate models suggest that by the end of this century it could attain levels that have recently driven the breakup of ice shelves around the Antarctic Peninsula (Trusel et al., 2015).

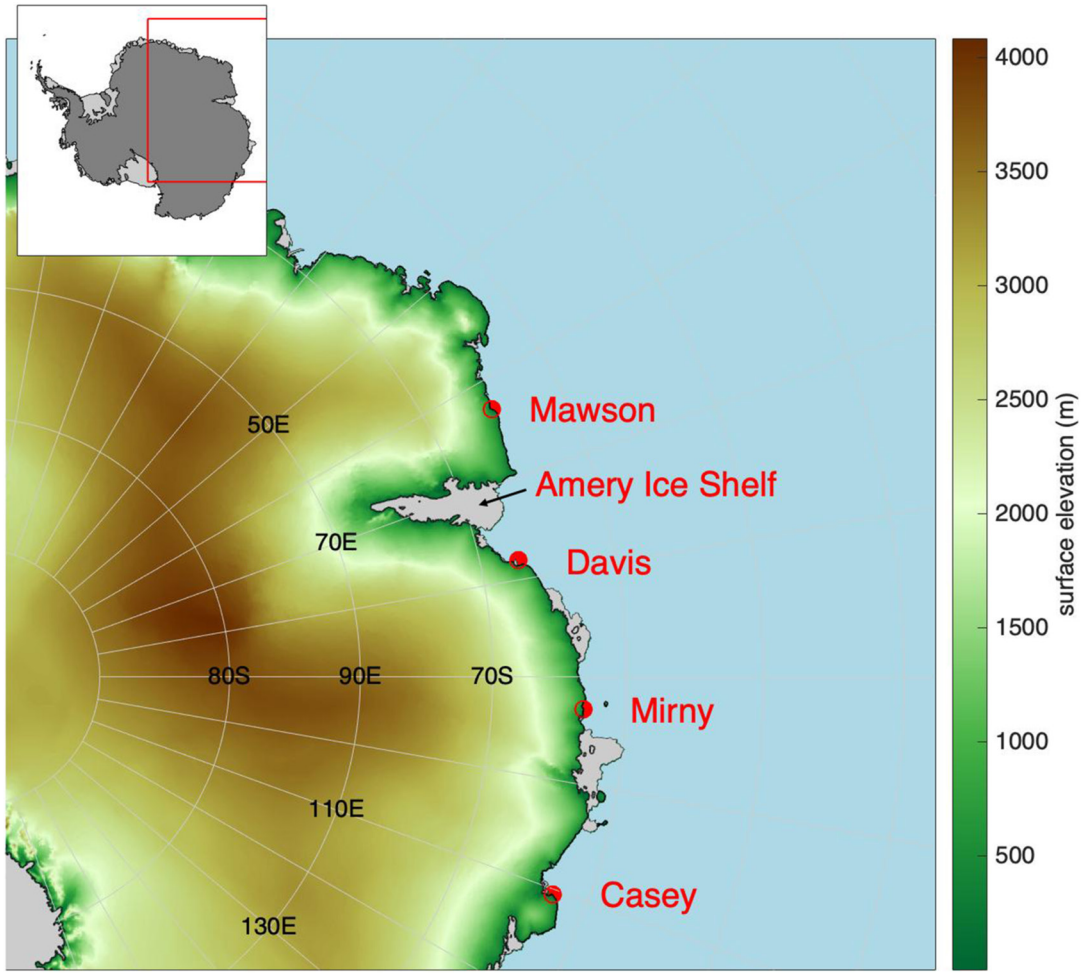

Figure 1. Map of Antarctic orography with station locations.

To date there have been few investigations into high temperature events in East Antarctica. Sinclair (1981) examined a case in December 1978 when record high temperatures were recorded at several East Antarctic coastal stations, including Davis (Figure 1) where the temperature rose to 10.0°C.

Recently, Robinson et al. (2020) considered a record high temperature event at Casey. This was a relatively long-lived event with large positive day- and night-time temperature anomalies from 23–26 January 2020. The event satisfied the criterion of a "heat wave", defined as three consecutive days with both extreme maximum and minimum temperatures (e.g., Faye et al., 2021).

Some high temperatures in the Antarctic coastal region have been linked to atmospheric rivers, which are narrow bands of warm, moist air originating in mid- or low-latitudes (Gorodetskaya et al., 2014; Wille et al., 2019). Typically, a ridge downstream of the river directs lower-latitude moisture flow toward the Antarctic (Terpstra et al., 2021). On average 12 atmospheric rivers occurred each year during 1979–2017 in the coastal region of West Antarctica, with these giving positive surface temperature anomalies of 4-5°C and extensive surface melt (Wille et al., 2019; Zou et al., 2021a, 2021b).

While we expect to see more extreme high temperatures across Antarctica in the coming decades as greenhouse gas concentrations increase, over the instrumental period there was only an increase in extreme high temperatures at stations on the Antarctic Peninsula in the second half of the Twentieth Century (Turner et al., 2021). This was followed by fewer extremes as there was a general cooling across the region, although some individual record high temperatures were recorded, such as the temperature of 18.3°C at Esperanza on 6 February 2020 (Francelino et al., 2021).

Here we investigate one extreme high temperature event that was associated with a pool of very warm air in early December 1989 when an atmospheric river transported low-latitude air into the Antarctic coastal region. The temperatures rose to record levels with positive lower tropospheric temperature anomalies of >14°C when adiabatic warming inland of the coast occurred during a period of downslope flow of record summer strength.

2. Data and Methods

We use surface and upper air observations made as part of the routine meteorological observing programs. Three hourly surface observations were available from Mawson (67.6°S, 62.87°E, from 1954), Davis (68.58°S, 77.97°E, from 1957) and Casey (66.3°S, 110.5°E, from 1959), with 6-hourly data for Mirny (66.56°S, 93.00°E, from 1956). Radiosonde ascents were available each day at 00 UTC from Mawson and at 00 and 12 UTC from Davis and Mirny. The daily maximum and minimum thermograph temperatures and full meteorological register data are available for Mawson, Davis and Casey, but not from Mirny. No automatic weather stations were operational near the warm pool at the time of the event.

Atmospheric circulation was examined using the ERA5 reanalysis fields produced by the European Centre for Medium-range Weather Forecasts (Hersbach et al., 2020) as it has been shown that these have a good representation of temperatures across the Antarctic (Gossart et al., 2019). A comparison of the Mawson 700 hPa radiosonde temperatures and the ERA5 reanalysis at the location of Mawson (Figure S1a in Supporting Information S1), indicates that the reanalysis fields had a good representation of the warming at this location. Surface and upper-air fields were available every hour, along with the daily precipitation total. Because of the smoothed orography there are some differences between the station data and reanalysis fields, especially near the surface. For example, Mawson station has an elevation of 16 m, but the "surface" in ERA5 at this location is at 353 m, resulting in the ERA5 surface temperatures being on average 3°C colder than the station data (Figure S1b in Supporting Information S1). Anomalies of model and station data were calculated by subtracting the mean values computed over the 30-year base period of 1980–2009.

The location of the atmospheric river was tracked using the ERA5 integrated water vapor (IWV). The atmospheric river detection algorithm searches for regions of vIVT (the meridional component of integrated vapor transport (see Wille et al., 2019 for details)) between 37.5°S and 80°S that exceed the 98th percentile of all monthly vIVT values per grid cell from 1980 to 2021. If the algorithm detects a band of vIVT values above this threshold that extends at least 20° in the meridional direction, that band is classified as an atmospheric river. See Wille et al. (2021) for further details. Polar orbiting satellite IR images were used to follow the evolution of the cloud features.

Thermal advection was estimated as $-\mathbf{v}.\nabla_I T$ using hourly isentropic level data where $\mathbf{v}$ is the horizontal wind vector and T is temperature and the subscript indicates an isentropic surface. Determining thermal advection on isentropic surfaces allows us to obtain quantitative estimates of vertical motion and to coherently track the 3-dimensional transport of heat and moisture in space and time. We particularly focus on thermal advection on the 300 K isentropic surface as this is close to 700 hPa where the greatest warming occurred and where the level is above the orography in the coastal region.

3. Extreme Temperatures in the In-Situ Data

Mean 1980–2009 December surface temperatures for the stations considered here are −0.7°C (Mawson), 0.1°C (Davis), −2.7°C (Mirny) and −1.1°C (Casey). Several near-record surface and upper-air temperatures were recorded in early December 1989. The highest surface temperatures reported at standard synoptic hours were 8.1°C at Mawson (12 UTC 5 December, the second highest temperature in the record), 9.2°C at Davis (12 UTC 4 December, the 9th highest temperature), 5.1°C at Casey (00 UTC 4 December, the 44th highest temperature in the record) and 1.5°C at Mirny (12 UTC 4 December, much lower than the station record high of 6.7°C at 6 UTC 2 January 1998). The highest maximum thermograph temperatures were 9.3°C at Mawson (approximately 17:00 UTC 5 December, the second highest thermograph measurement in the record), 10.1°C at Davis (5 December, the 12th highest) and 6.6°C at Casey (the 29th highest, although the thermograph records at the station only start in 1989).

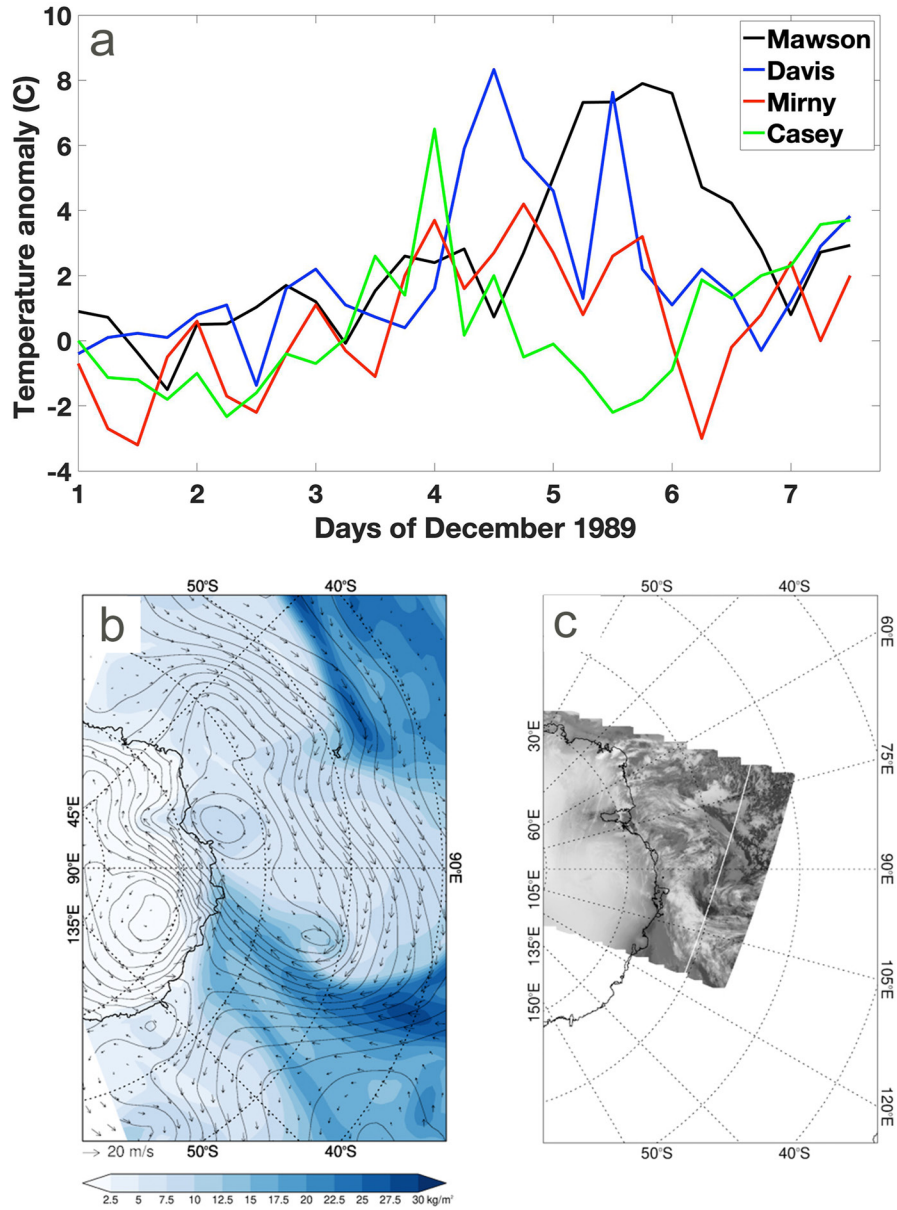

Figure 2. (a) 2 m air temperature anomalies for the four stations, (b) IWV (colors), MSLP (contour lines) and 10 m wind vectors at 00 UTC 3 December 1989 and (c) NOAA-10 IR satellite image at 23:19 UTC 1 December 1989.

The four stations all experienced an increase in surface temperature anomaly of several degrees between 00 UTC 1 December and 00 UTC 4 December (Figure 2a). This was followed by a sharp peak in the temperature anomaly that broadly affected the stations from east to west, arriving at 00 UTC 4 December (Casey, +6.5°C anomaly), 18 UTC 4 December (Mirny, +4.2°C anomaly), 12 UTC 4 December (Davis, +8.3°C anomaly with a secondary peak of +7.6°C at 12 UTC 5 December) and 18 UTC 5 December (Mawson, +7.9°C anomaly; Figure 2a).

The 700 hPa radiosonde temperatures indicate a more gradual increase during the first week of December, but there were still some substantial temperature rises during the event of up to 15°C at the stations (e.g., Mawson, Figure S1a in Supporting Information S1). The peak in 700 hPa temperature passed from east to west, being registered in the radiosonde data at 00 UTC 3 December for Casey (−7.7°C), 00 UTC 3 December for Mirny (−9.3°C), 00 UTC 5 December for Davis (−5.8°C) and 00 UTC 6 December for Mawson (−5.0°C). The 700 hPa temperatures were most extreme in the western part of the region, with the Mawson 700 hPa temperature being

the third highest in the record. Further to the east the temperatures were in the top 0.2%, 1.8% and 1.1% of summer records at Davis, Mirny and Casey respectively.

4. The Impact of Strong Thermal Advection and the Atmospheric River

During early December the area north of the Amery Ice Shelf (AIS; Figure 1) was characterized by a quasi-stationary, multi-centered surface low pressure system (e.g., Figure 2b) and associated upper-level trough (Figure S2 in Supporting Information S1), with a ridge of high pressure further to the east.

East of the low center there was strong northerly flow, with the satellite imagery showing a cloud band lying along the coast by 23 UTC 1 December (Figure 2c), indicating a warm front at the boundary between warm low-latitude air and a cold continental airmass. Early on 2 December the horizontal thermal advection was greatest near the warm front. This led to 700 hPa temperatures rising to the east of the AIS with temperature anomalies of >+8°C on the coast at 100°E by 18 UTC 2 December.

The upper-level trough amplified during 2 December and a deep surface low formed close to 50°S, 105°E by 00 UTC 3 December (Figure 2b), while the ridge built toward the south. The ridge was associated with a band of air with small negative values of PV that extended from the east and north on the 300 K surface (Figure S3b in Supporting Information S1).

There was substantial horizontal warm advection in the northerly flow and transport of moist air toward the Antarctic from as far north as 40°S. An atmospheric river was detected extending from the southwestern tip of Australia to the landfall location between Davis and Casey over 00 UTC 2 December and 3 December 18 UTC (Figure S4 in Supporting Information S1). The IWV field (Figure 2b) highlights the atmospheric river as a long, narrow band of moist air lying along the 110°E meridian to the east of cold air that had circulated around the large area of low pressure. This scenario resulted in >25 mm of precipitation near the coast at 100°E according to ERA5.

By 3 December the warm air had penetrated inland across the coastal area between Mirny and the AIS, with Mirny and Casey recording their highest 700 hPa radiosonde temperatures during the event of −9.3°C and −7.7°C respectively at 00 UTC 3 December. Warm air penetration from lower latitudes can also be seen in the 300 K PV fields (Figure S3b in Supporting Information S1). At this time there was the largest horizontal warm advection for the event (Figure 3a) and on 3 December there was >40 mm of precipitation just inland of the coast at 95°E.

Strong 300 K thermal advection continued into 4 December and close to the AIS (70°S, 75°E) it reached a maximum of 4.65×10^{-4} K s^{-1} at 06 UTC, which was within the highest 1% of advection values at this location. This took place when the frontal cloud band was over the AIS and winds were from the northeast. There will have been some heating because of diabatic processes, but this was likely insignificant compared to the warming by thermal advection. Despite the strong thermal advection, the 700 hPa temperature only rose to −11.8°C by 06 UTC 4 December (an anomaly of +6.2°C), a level that is attained in most summers above the AIS. However, at the surface the 2 m temperature had increased to 2.3°C by this time, which was the 16th highest near-surface temperature at this location. The surface temperature began to increase at 12 UTC 3 December when the 10 m wind started to turn toward the southeast. In contrast, the 700 hPa wind direction remained from the northeast until 06 UTC 4 December, delaying the increase of temperature compared to the surface layer.

Early on 4 December the surface winds backed parallel to the coast and the strongest coastal easterlies were experienced, with the reanalysis having a 700 hPa easterly wind component of 31 m s^{-1} at 65°S, 90°E at 12 UTC. At this time the Mirny radiosonde 700 hPa wind speed was 27.4 m s^{-1}, which was strong, but not exceptional.

The frontal cloud band still lay along the coast from 90°E to the eastern side of the AIS (Figure 3b), showing a well-defined north-south separation between the low-latitude and continental air. This boundary is also apparent in the ERA5 PV field from 00 UTC 4 December (Figure S3c in Supporting Information S1), indicating that warm air became confined to the south and east of the front. The ERA5 data showed ascent along the frontal cloud band and descent further inland. Climatologically, there is downslope flow in this sector from the high plateau and a belt of descending air just inland of the coast. This circulation is strongest in winter, when it is associated with persistent katabatic winds, but is still present during summer. The diurnal cycle of low-level temperature is important for the generation of katabatic winds in the summer, as is the background temperature gradient between

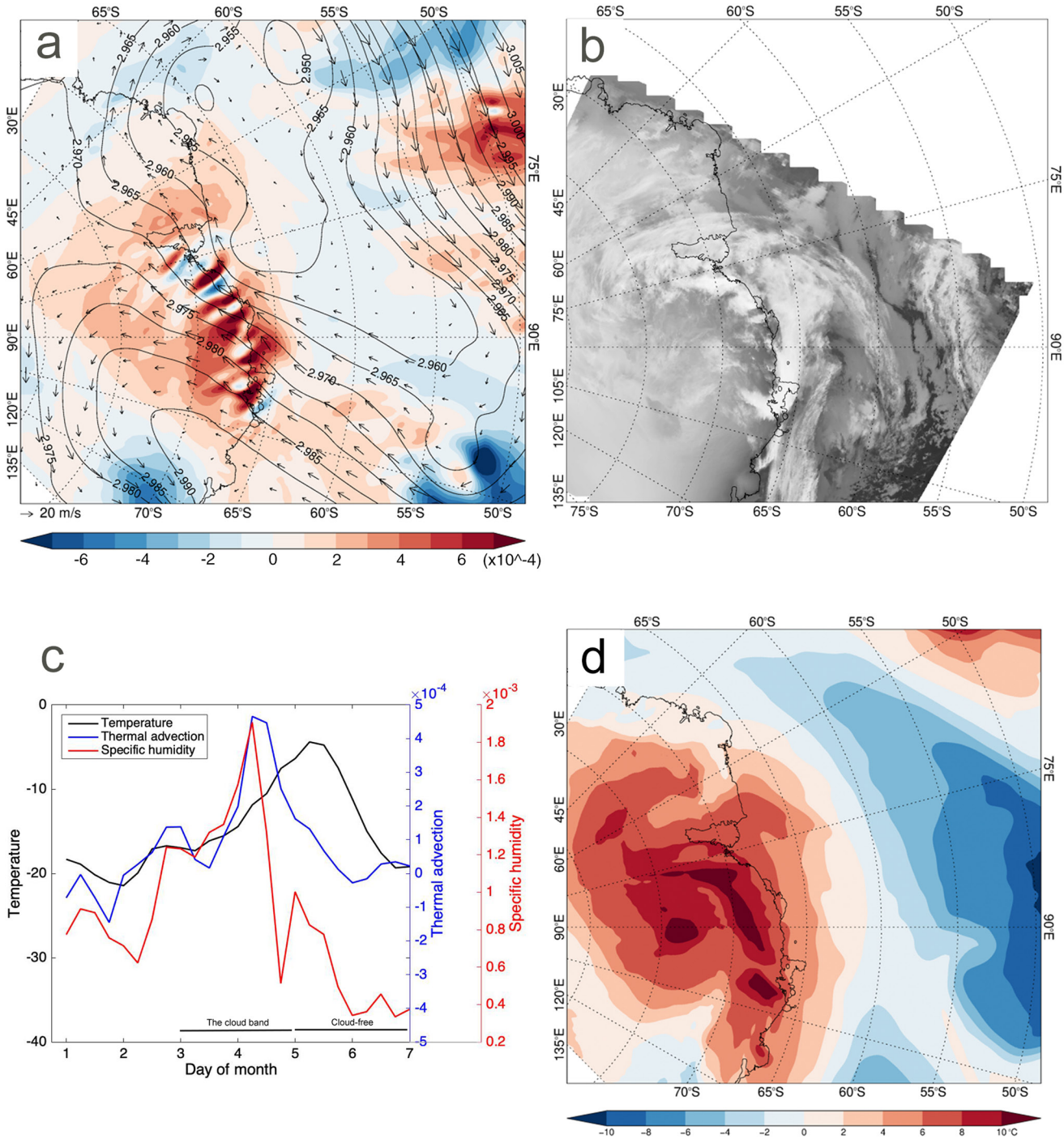

Figure 3. (a) Horizontal thermal advection on the 300 K surface (with the magnitude shown on the scale) and the 300 K Montgomery potential and wind vectors at 00 UTC 3 December, (b) IR satellite image at 23 UTC 3 December, (c) 700 hPa temperature, 700 hPa specific humidity and 300 K thermal advection for the first 7 days of December 1989 at 70°S, 75°E and (d) 700 hPa temperature anomaly at 12 UTC 4 December 1989.

the cold continent air and relatively warm conditions over the ocean (Parish & Cassano, 2001). At 00 UTC 4 December the vertical velocities just inland of the coast were close to the climatological mean (not shown) but started to increase after this time.

5. Strong Downslope Flow and Westward Track of the Warm Pool

The 4 December was the key day in the development of the warm pool when the 700 hPa temperature on the eastern side of the AIS at 70°S, 75°E increased by 8.1°C - the largest 24-hr temperature increase at this location during the event and the third largest December 24-hr warming in the record. At 12 UTC there were strong easterly winds east of the AIS with the Mirny radiosonde 850 hPa wind at this time being 36 m s^{-1}, which was the sixth highest December speed at this level in the record. The downslope flow from the interior of the continent was also very strong, corresponding to a confined region of less negative PV (indicating warmer air) with an anticyclonic circulation centered at 70°S, 100°E (Figure S3c in Supporting Information S1). In the easterly flow the frontal cloud band was rapidly advected toward the west, clearing the AIS between 00 and 12 UTC. This corresponded with a large decrease of 700 hPa specific humidity as the dry, continental air extended over the area (Figure 3c). The passage of the front was also reflected in the decrease of cloud at Davis, which dropped to 0 oktas by 12 UTC 4 December when the station recorded a surface temperature of 9.2°C, which was the highest standard hour temperature at the site during the event.

Strong horizontal warm advection was the dominant factor in the increase of temperature over the AIS up to 12 UTC 4 December, when the warm pool became isolated from colder, low latitude air to the north. This dynamical isolation from lower latitude airmasses is also apparent in the less negative PV (i.e., warmer air) southeast of the AIS. This feature had an anticyclonic circulation that gradually moved westward (Figures S3c–S3f in Supporting Information S1).

At 12 UTC 4 December the largest 700 hPa temperature anomalies of >+10°C were found in an arc inland southeast of the AIS (Figure 3d), with the anomalies coinciding with the largest 700 hPa descent on the poleward side of the front (Figure S5 in Supporting Information S1). After 12 UTC 4 December the surface winds at 70°S, 75°E veered from northeast to southeast. Up to this time the temperature anomalies increased at a similar rate at all levels up to 500 hPa, but subsequently the anomalies increased most at lower levels and especially at 700 hPa where they rose until 06 UTC 5 December (Figure S6 in Supporting Information S1).

As pressure over the continent rose while remaining low over the ocean, the pressure gradient became stronger across the interior and the wind speeds rose. The area 70–85°S, 90–130°E has a mean December 10 m wind speed of 4.3 m s^{-1}, but increased to 12.7 m s^{-1} at 06 UTC 5 December (Figure 4a), which was the highest December speed for this area in the reanalysis period. As the downslope winds increased, the rate of descent of lower tropospheric air rose. At 68°S, 96.5°E the mean December 700 hPa vertical velocity is 0.45 Pa s^{-1}, however, in December 1989 this reached a maximum of 2.04 Pa s^{-1} at 06 UTC 5 December (Figure 4b), which was within the highest 2% of December vertical velocities at this location. At 70°S, 75°E the vertical velocities switched from ascent to descent following the passage of the front early on 4 December, with the greatest descent being 0.83 Pa s^{-1} at 700 hPa at 10 UTC 5 December.

The coastal easterly winds were still very strong on 5 December (the 00 UTC Mirny radiosonde 700 hPa wind speed was 21.5 m s^{-1}) and the cloud band marking the leading edge of the continental air moved rapidly west leading to cloud-free conditions across the AIS (Figure 4c). The cloud cover at Mawson dropped from 6 okta at 00 UTC to 1 oktas by 9 UTC and between 06 and 12 UTC the surface temperature rose by 5°C following the clearance of the cloud.

During the day the band of coastal descent also translated to the west. Above the AIS the 700 hPa temperature at 06 UTC 5 December reached −4.4°C (anomaly >14°C, Figure 4d), which was the highest temperature at that location in the whole reanalysis record. At this time the surface temperature anomalies were >8°C across the area inland of the coast from 60° to 80°E.

The largest surface temperature anomalies were located in a band from Mawson to the western AIS at 18 UTC 5 December, close to the time that the highest temperature of +9.3°C was recorded at Mawson at approximately 17 UTC 5 December. With air temperatures above freezing across a large area on 5 December the SSM/I data indicated significant surface melt. There had been some surface melt at well-separated locations along the coast during the first 4 days of December (Figure S7 in Supporting Information S1). However, as surface temperatures increased on the 5 December the melt extended to the whole of the AIS and along the coast to the east and west of Mirny. The melt continued in these area on 6 December and also occurred to the west of Mawson as the warm pool extended westwards.

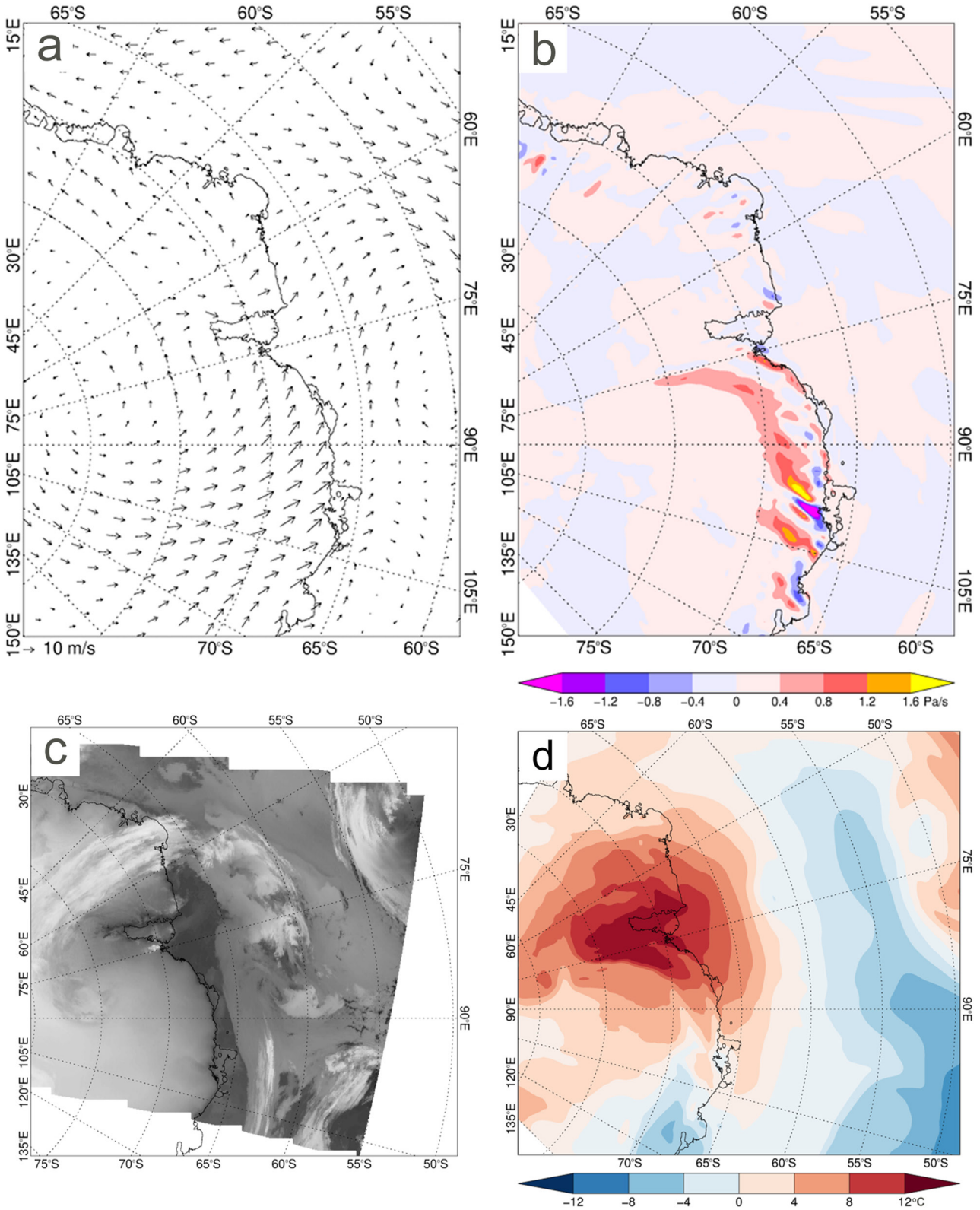

Figure 4. (a) 10 m wind vectors at 06 UTC 5 December 1989, (b) the 700 hPa vertical velocity at 06 UTC 5 December 1989, (c) IR satellite image at 23 UTC 4 December 1989 and (d) 700 hPa temperature anomaly at 06 UTC 5 December 1989.

During 6 December the high over the interior declined and the strong flow from the interior reduced, with the winds backing to a strong easterly. The large 700 hPa temperature anomaly of >14°C was still present just inland of Mawson at 00 UTC 6 December but gradually decreased during the day and moved north – the development and track of the warm pool throughout the event can be seen in Figure S8 in Supporting Information S1. An area of strong cold air advection moved eastwards over the AIS and cold air flowed north off this sector of the continent, signaling the end of the event.

6. Summary and Discussion

The short period of very high temperatures affecting coastal East Antarctic in early December 1989 was a very rare event as evidenced by the fact that Mawson recorded its second highest temperature. Two unusual atmospheric conditions came together to give the high temperatures. First, there was sustained warm advection into the region within an atmospheric river. Second, there were exceptional summer downslope winds, which promoted strong descent of mid-tropospheric air leading to further warming.

Storm activity in the circumpolar trough is at a minimum during summer (Jones & Simmonds, 1993), but very deep unseasonal depressions do occur occasionally, advecting warm air toward the Antarctic. However, many are mobile systems that do not give sustained southward warm advection. The depression located near 50°S, 105°E in early December 1989 had a central pressure of ~963 hPa, which was not exceptional, but its quasi-stationary nature coupled with high pressure to the east led to strong warm advection.

Atmospheric rivers are relatively rare events in this sector of the Southern Ocean with normally just three or four each year. The northerly flow in early December 1989 gave horizontal warm advection on the 300 K surface toward the AIS that was within the highest 1% during the reanalysis period at that location, indicating that sustained transport of this magnitude is very rare. But the temperature above the AIS was only −11.8°C at 6 UTC 4 December. However, further warming occurred during strong downslope flow during 4 December in association with a cut-off high with an airmass that originated in low latitudes. In fact, the areal 24-hr averaged PV at 300 K over 68–80°S, 60–100°E from 18 UTC 4th to 12 UTC 5th December 1989 was the highest for December in this area. The 500 hPa geopotential height of 5,368 m at 75°S, 90°E on 06 UTC 4 December 1989 was within the highest 1.3% of December 500 hPa heights at this location and, with a low of moderate depth off the coast, led to the very strong downslope flow, descent in the coastal zone and adiabatic warming. This increased the 700 hPa temperature at 70°S, 75°E to −4.4°C at 06 UTC 5 December, which was the highest in the whole record starting in 1979. Casey and Mirny, were the only stations influenced by the atmospheric river. In contrast, Mawson and Davis were influenced by both the atmospheric river and the warm pool following the period of strong downslope flow from the interior.

Climatologically, the highest December 700 hPa temperatures above the AIS occur with a 500 hPa high inland and a low to the northeast (Figure S9a in Supporting Information S1). The mean 500 hPa geopotential height field for 48 hr before the maxima (Figure S9b in Supporting Information S1) has the high developing from a ridge extending from the northeast, and northeasterly flow toward the AIS with warm air reaching the coast east of the AIS. This was basically the scenario in which the December 1989 event occurred (Figures S9d–S9f in Supporting Information S1), but there was a much more well-developed cold trough to the west of the warm tongue in 1989 with stronger northerly flow that led to the very strong horizontal thermal advection. During the highest temperatures above the AIS, there is a southeasterly flow across the area to the east of the AIS (Figure S9a in Supporting Information S1), but this was much stronger than usual on 5 December 1989 (Figure S9d in Supporting Information S1).

While the two highest 700 hPa temperatures at 70°S, 75°E occurred on 5 December 1989, the third to the seventh highest were during 27–28 December 1989. The later warming started on 26 December (Figure S10 in Supporting Information S1) when there was strong northerly flow between a low to the west of the ice shelf and a ridge to the east. As with the earlier event, the strong warm advection from the north switched to a strong southeast flow on the 27 December as temperatures rose to near-record high temperatures.

It is very unusual to have two extreme high temperature events in the region in 1 month. Both were associated with the same pattern of strong warm advection, followed by marked downslope flow as the ridge became an isolated high inland of the AIS. However, not all warm ridges give record temperatures. On occasions ridges

developed toward the AIS from longitudes close to 160°E but these don't lead to strong flow from the interior, so the temperatures do not reach extreme levels. The 500 hPa heights along the Antarctic coast near 120°E in December 1989 were higher than in any other December in the record starting in 1979. Marked ridging in this sector is not related to tropical climate variability or the modes of high southern latitude climate variability and the occurrence of the two high temperature events appears to have arisen because of a rare combination of synoptic events.

Data Availability Statement

The station surface and upper air observations are available at https://legacy.bas.ac.uk/met/READER/ANTARCTIC_METEOROLOGICAL_DATA/SURFACE/surface_index.html and https://legacy.bas.ac.uk/met/READER/ANTARCTIC_METEOROLOGICAL_DATA/UPPER_AIR/upper_air_index.html respectively. The ERA5 hourly fields are available from the Copernicus Climate Data Store, https://doi.org/10.24381/cds.bd0915c6. The daily fields of surface ice melt are available at https://ramadda.data.bas.ac.uk/repository/entry/show/?entryid=ffd24dd7-e201-4a02-923f-038680bf7bb5.

Acknowledgments
This work forms part of the Polar Science for Planet Earth program of the British Antarctic Survey. We are grateful to ECMWF for the provision of the ERA5 meteorological fields. It contains modified Copernicus Climate Change Service information 2021. Neither the European Commission nor ECMWF is responsible for any use that may be made of the Copernicus information or data it contains. The datasets Hersbach (2018a); Hersbach (2018b) were downloaded from the Copernicus Climate Change Service (C3S) Climate Data Store. Matthew Lazzara was supported by the National Science Foundation Grant No. 1951603.

References

Bamber, J. L., Oppenheimer, M., Kopp, R. E., Aspinall, W. P., & Cooke, R. M. (2019). Ice sheet contributions to future sea-level rise from structured expert judgment. *Proceedings of the National Academy of Sciences*, *116*, 11195–11200. https://doi.org/10.1073/pnas.1817205116

Dutrieux, P., De Rydt, J., Jenkins, A., Holland, P. R., Ha, H. K., Lee, S. H., et al. (2014). Strong sensitivity of Pine Island Ice-Shelf melting to climatic variability. *Science*, *343*, 174–178. https://doi.org/10.1126/science.1244341

Faye, M., Dème, A., Diongue, A. K., & Diouf, I. A. (2021). Impact of different heat wave definitions on daily mortality in Bandafassi, Senegal. *PLOS ONE*, *16*, e0249199. https://doi.org/10.1371/journal.pone.0249199

Francelino, M. R., Schaefer, C., Colwell, S., Brunet, M., Renwick, J., Jones, P., et al. (2021). WMO evaluation of two extreme high temperatures occurring in February 2020 for the Antarctic Peninsula region. *Bulletin of the American Meteorological Society*, *102*, E2053–E2061. https://doi.org/10.1175/BAMS-D-21-0040.1

Gorodetskaya, I. V., Tsukernik, M., Claes, K., Ralph, M. F., Neff, W. D., & van Lipzig, N. P. M. (2014). The role of atmospheric rivers in anomalous snow accumulation in East Antarctica. *Geophysics Research Letters*, *41*, 6199–6206. https://doi.org/10.1002/2014GL060881

Gossart, A., Helsen, S., Lenaerts, J. T. M., Vanden Broucke, S., van Lipzig, N. P. M., & Souverijns, N. (2019). An evaluation of surface climatology in state-of-the-art reanalyses over the Antarctic ice sheet. *Journal of Climate*, *32*(20), 6899–6915. https://doi.org/10.1175/jcli-d-19-0030.1

Herraiz-Borreguero, L., Coleman, R., Allison, I., Rintoul, S. R., Craven, M., & Williams, G. D. (2015). Circulation of modified circumpolar deep water and basal melt beneath the Amery ice shelf, East Antarctica. *Journal of Geophysical Research: Oceans*, *120*(4), 3098–3112. https://doi.org/10.1002/2015JC010697

Hersbach, H., Bell, B., Berrisford, P., Biavati, G., Horányi, A., Muñoz Sabater, J., et al. (2018a). *ERA5 hourly data on single levels from 1979 to present, Copernicus climate Change Service (C3S) climate data Store (CDS)*. https://doi.org/10.24381/cds.adbb2d47

Hersbach, H., Bell, B., Berrisford, P., Biavati, G., Horányi, A., Muñoz Sabater, J., et al. (2018b). *ERA5 hourly data on pressure levels from 1979 to present, Copernicus Climate Change Service (C3S) Climate Data Store (CDS)*. https://doi.org/10.24381/cds.bd0915c6

Hersbach, H., Nicolas, J., Peubey, C., Berrisford, P., Hirahara, S., Bell, B., et al. (2020). The ERA5 global reanalysis. *Quarterly Journal of the Royal Meteorological Society*, *146*(730), 1999–2049.

Jones, D. A., & Simmonds, I. (1993). A climatology of Southern Hemisphere extratropical cyclones. *Climate Dynamics*, *9*, 131–145. https://doi.org/10.1007/bf00209750

Levermann, A., Winklemann, R., Albrecht, T., Goelzer, H., Golledge, N. R., Greve, R., et al. (2020). Projecting Antarctica's contribution to future sea level rise from basal ice shelf melt using linear response functions of 16 ice sheet models (LARMIP-2). *Earth System Dynamics*, *11*(1), 35–76. https://doi.org/10.5194/esd-11-35-2020

Nowicki, S., & Seroussi, H. (2018). Projections of future sea level contributions from the Greenland and Antarctic ice sheets: Challenges beyond dynamical ice sheet modeling. *Oceanography*, *31*, 109–117. https://doi.org/10.5670/oceanog.2018.216

Parish, T. R., & Cassano, J. J. (2001). Forcing of the wintertime Antarctic boundary layer winds from the NCEP-NCAR global reanalysis. *Journal of Applied Meteorology*, *40*(4), 810–821. https://doi.org/10.1175/1520-0450(2001)040<0810:fotwab>2.0.co;2

Park, J. W., Gourmelen, N., Shepherd, A., Kim, S. W., Vaughan, D. G., & Wingham, D. J. (2013). Sustained retreat of the Pine island Glacier. *Geophysical Research Letters*, *40*(10), 2137–2142. https://doi.org/10.1002/grl.50379

Pritchard, H. D., Ligtenberg, S. R. M., Fricker, H. A., Vaughan, D. G., Van den Broeke, M. R., & Padman, L. (2012). Antarctic ice-sheet loss driven by basal melting of ice shelves. *Nature*, *484*(7395), 502–505. https://doi.org/10.1038/nature10968

Rignot, E., Mouginot, J., Scheuchl, B., Van den Broeke, M., Van Wessem, J. M., & Morlighem, M. (2019). *Four decades of Antarctic ice sheet mass balance from 1979–2017* (Vol. 116). Proceedings of the National Academy of Sciences of the United States of America. https://doi.org/10.1073/pnas.1812883116

Robinson, S. A., Klekociuk, A. R., King, D. H., Rojas, M. P., Zuniga, G. E., & Bergstrom, D. M. (2020). The 2019/2020 summer of Antarctic heatwaves. *Global Change Biology*, *26*(6), 3178–3180. https://doi.org/10.1111/gcb.15083

Sinclair, M. R. (1981). Record-high temperatures in the Antarctic - A synoptic case study. *Monthly Weather Review*, *109*, 2234–2242. https://doi.org/10.1175/1520-0493(1981)109<2234:rhtita>2.0.co;2

Tedesco, M. (2009). Assessment and development of snowmelt retrieval algorithms over Antarctica from K-band spaceborne brightness temperature (1979–2008). *Remote Sensing of Environment*, *113*(5), 979–997. https://doi.org/10.1016/j.rse.2009.01.009

Terpstra, A., Gorodetskaya, I. V., & Sodemann, H. (2021). Linking sub-tropical evaporation and extreme precipitation over East Antarctica: An atmospheric river case study. *Journal of Geophysical Research: Atmospheres*, *126*(9), e2020JD033617. https://doi.org/10.1029/2020JD033617

Trusel, L. D., Frey, K. E., Das, S. B., Karnauskas, K. B., Kuipers Munneke, P., van Meijgaard, E., & van den Broeke, M. R. (2015). Divergent trajectories of Antarctic surface melt under two twenty-first-century climate scenarios. *Nature Geoscience*, *8*(12), 927–932. https://doi.org/10.1038/ngeo2563

Turner, J., Lu, H., King, J. C., Marshall, G. J., Phillips, T., Bannister, D., & Colwell, S. (2021). Extreme temperatures in the Antarctic. *Journal of Climate*, *34*, 2653–2668. https://doi.org/10.1175/jcli-d-20-0538.1

Turner, J., Orr, A., Gudmundsson, G. H., Jenkins, A., Bingham, R. G., Hillenbrand, C. D., & Bracegirdle, T. J. (2017). Atmosphere-ocean-ice interactions in the Amundsen Sea embayment, West Antarctica. *Reviews of Geophysics*, *55*, 235–276. https://doi.org/10.1002/2016RG000532

Wille, J. D., Favier, V., Dufour, A., Gorodetskaya, I. V., Turner, J., Agosta, C., & Codron, F. (2019). West Antarctic surface melt triggered by atmospheric rivers. *Nature Geoscience*, *12*, 911–916. https://doi.org/10.1038/s41561-019-0460-1

Wille, J. D., Favier, V., Gorodetskaya, I. V., Agosta, C., Kittel, C., Beeman, J. C., et al. (2021). Antarctic atmospheric river climatology and precipitation impacts. *Journal of Geophysical Research: Atmospheres*, *126*(8), e2020JD033788. https://doi.org/10.1029/2020JD033788

Zou, X., Bromwich, D. H., Montenegro, A., Wang, S. H., & Bai, L. S. (2021a). Major surface melting over the Ross Ice Shelf part II: Surface energy balance. *Quarterly Journal of the Royal Meteorological Society*, *147*(738), 2895–2916. https://doi.org/10.1002/qj.4105

Zou, X., Bromwich, D. H., Montenegro, A., Wang, S. H., & Bai, L. S. (2021b). Major surface melting over the Ross Ice Shelf part I: Foehn effect. *Quarterly Journal of the Royal Meteorological Society*, *147*(738), 2874–2894. https://doi.org/10.1002/qj.4104